

On the Origin of the Kinematical Differences Between the Stellar Halo and the Old Globular Cluster System in the Large Magellanic Cloud

Kenji Bekki^{1*}

¹*School of Physics, University of New South Wales, Sydney 2052, NSW, Australia*

Accepted, Received 2005 February 20; in original form

ABSTRACT

We discuss structural and kinematical properties of the stellar halo and the old globular cluster system (GCS) in the Large Magellanic Cloud (LMC) based on numerical simulations of the LMC formation. We particularly discuss the observed possible GCS's rotational kinematics ($V/\sigma \sim 2$) that appears to be significantly different from the stellar halo's one with a large velocity dispersion ($\sim 50 \text{ km s}^{-1}$). We consider that both halo field stars and old GCs can originate from low-mass subhalos virialized at high redshifts ($z > 6$). We investigate the final dynamical properties of the two old components in the LMC's halo formed from merging of low-mass subhalos with field stars and GCs. We find that the GCS composed of old globular clusters (GCs) formed at high redshifts ($z > 6$) has little rotation ($V/\sigma \sim 0.4$) and structure and kinematics similar to those of the stellar halo. This inconsistency between the simulated GCS's kinematics and the observed one is found to be seen in models with different parameters. This inconsistency therefore implies that if old, metal-poor GCs in the LMC have rotational kinematics, they are highly unlikely to originate from the low-mass subhalos that formed the stellar halo. We thus discuss a scenario in which the stellar halo was formed from low-mass subhalos with no/few GCs whereas the GCS was formed at the very early epoch of the LMC's disk formation via dissipative minor and major merging of gas-rich subhalos and gas infall. We also discuss whether old GCs in the LMC can be slightly younger than the Galactic counterparts. We suggest that there can be a threshold subhalo mass above which GCs can be formed within subhalos at high redshifts and thus that this threshold causes differences in physical properties between stellar halos and GCSs in less luminous galaxies like the LMC.

Key words: galaxies: star clusters – globular clusters: general – galaxies: formation

1 INTRODUCTION

Structural, kinematical, chemical properties of the Large Magellanic Cloud (LMC) have been investigated by many authors concerning different stellar populations and gaseous components and suggested to have valuable information on formation and evolution history of the LMC (Hartwick & Cowley 1988; Meatheringham et al. 1988; Irwin 1991; Luks & Rohlfs 1992; Kunkel et al. 1997; Graff et al. 2000; Olsen & Salyk 2002; van den Marel et al. 2002; Cioni & Habing 2003; Staveley-smith et al. 2003; Cole et al. 2005). Previous numerical studies on dynamical and chemical evolution of the LMC compared the results with these observations and thereby tried to provide reasonable physical explanations

for the observations (e.g., Bekki et al. 2004; Bekki & Chiba 2005). Since these studies focused mainly on the origin of disk components of the LMC, the origin of the old stellar halo and the globular cluster system (GCS) composed of old, metal-poor globular clusters (GCs) remains unclear.

Recent observations have reported that the stellar halo of the LMC has a projected radial density profile similar to an exponential one (e.g., Alves 2004) and a larger velocity dispersion with possibly little rotation (Minniti et al. 2003; Gratton et al. 2004). The dynamically hot nature of the LMC's stellar halo has been confirmed by Borissova et al. (2006), which found that the stellar halo composed of RR Lyrae stars has the mean velocity dispersion of $\sim 50 \pm 2 \text{ km s}^{-1}$ and a Gaussian metallicity distributions function with mean $[\text{Fe}/\text{H}] = -1.53 \pm 0.02 \text{ dex}$. Subramaniam (2006) investigated spatial distributions of RR Lyrae stars from the

* E-mail: bekki@phys.unsw.edu.au

Table 1. Model parameters and a brief summary of the results

model	$M_t (\times 10^{10} M_\odot)$ ^a	λ ^b	δ_i ^c	N_{\min} ^d	z_{trun} ^e	$(\frac{V}{\sigma})_{\text{FS}}$ ^f	$(\frac{V}{\sigma})_{\text{GC}}$ ^g
Standard	6.0	0.08	0.39	32	15	0.34	0.39
Low density	6.0	0.08	0.19	32	15	0.60	0.56
High threshold	6.0	0.08	0.39	1000	15	0.28	0.22
Low-z truncation	6.0	0.08	0.39	32	10	0.19	0.21

^a Initial total masses.

^b Initial spin parameters.

^c Initial over densities.

^d Minimum mass for halo identification.

^e The epoch of truncation of GC formation.

^f Final $\frac{V}{\sigma}$ for field stars (FS), where V and σ are the maximum rotational velocity and the central velocity dispersion, respectively in the simulated LMC halo. The mean value averaged for three projections (x - y , x - z , and y - z) is shown.

^g $\frac{V}{\sigma}$ for GCs.

catalogue by Soszynski et al. (2003) and found that the inner stellar halo can have a disk density distribution.

Previous observational studies on the kinematics of the GCS composed of old, metal-poor GCs in the LMC suggested that the GCS has a disk distribution and rotational kinematics with a small velocity dispersion (e.g., Freeman et al. 1983; Kinman et al. 1991; Schommer et al. 1992; Grocholski et al. 2006). It is suggested that it could be difficult to make a robust conclusion on the presence of the rotational kinematics owing to the small number (13) of the GCs (van den Bergh 2004). The total number of old, metal-poor GCs with $[\text{Fe}/\text{H}] < -1.3$ and well determined radial velocities are five in the sample of GCs by Grocholski et al. (2006), which implies that old GCs can have different kinematics from young and intermediate-age GCs with rotational kinematics. The observed possible rotational kinematics with $V/\sigma \sim 2$ (Schommer et al. 1992) however suggests that there is a significant kinematical difference in the stellar halo and the GCS composed of old GCs in the LMC. No theoretical explanations however have been proposed for the origin of this kinematical difference.

The purpose of this paper is to investigate the origin of the observed kinematical difference between the stellar halo and the GCS composed of old, metal-poor GCs in the LMC based on numerical simulations of the LMC formation. We here consider that the stellar halo and the GCS are formed from hierarchical merging of subhalos that are virialized before reionization and have both field stars and GCs. We therefore perform numerical simulations for the formation of the LMC based on the cold dark matter (CDM) model and thereby investigate structure and kinematics of the simulated stellar halo and GCS. By comparing the simulated kinematical properties of the stellar halo and the GCS with observations, we try to discuss the relationship between the stellar halo formation and GC one in the early history of the LMC.

The plan of the paper is as follows: In the next section, we describe our numerical models for the stellar halo and GC formation of the LMC. In §3, we present the numerical results mainly on the kinematics of the simulated halo and GCS for variously different models. In §4, we discuss a promising scenario explaining the observed kinematical difference between the old stellar halo and the GCS in the LMC. We summarize our conclusions in §5.

2 THE MODEL

2.1 GC formation

This paper is the first step toward better understanding structural, kinematical, and chemical properties of the LMC's GCS in a comprehensive way. Therefore we adopt a more idealized model of GC formation in the LMC that is assumed to be formed from hierarchical merging of low-mass subhalos. We adopt a model in which GCs (and field stars) are formed within subhalos virialized at high redshifts ($z > 6$). Although the adopted model of GC formation within subhalos at high redshifts has not been confirmed observationally (Brodie & Strader 2006 for different models of GC formation), recent numerical simulations based on the model have successfully explained some fundamental observations such as radial density profiles of GCSs (e.g., Santos 2003; Bekki 2005).

We consider that star formation and thus GC one can proceed at high redshifts only in virialized dark matter halos before reionization. The physical reason for the suppression of star formation by reionization is that ultraviolet background radiation in a reionized universe can significantly reduce the total amount of cold HI gas and molecular one (through photoevaporation/photoionization of the gas) that are observed to be indispensable for active star formation in low-mass galaxies (e.g., Young and Lo 1997). Recent high-resolution simulations on this issue (Susa & Umemura, 2004) have confirmed that significant suppression of the formation of cold gas can lead to the suppression of star formation in dwarf galaxies embedded in dark matter halos, in particular, lower-mass dwarfs. We here focus exclusively on very old, metal-poor GCs in the LMC, which could have formed at very high redshifts: it is, however, observationally unclear whether the GCs were formed before reionization. Therefore, it is reasonable to adopt the above assumption that GC formation can proceed in dark matter subhalos virialized before reionization.

Massive and dense star clusters like GCs are suggested to form in GMCs surrounded by high-pressure interstellar medium (ISM) in galaxies (Elmegreen & Efremov 1997). We therefore assume that GCs are formed in the very central regions of subhalos, where gaseous pressure should be so high owing to their deep gravitational potentials. During destruction of subhalos with GCs in the hierarchical growth of the

LMC, the GCs are stripped and dispersed into the halo to become the halo GCs in the LMC. This formation processes of GCs from low-mass galactic systems was demonstrated by previous numerical simulations (e.g., Bekki & Freeman 2003; Mizutani et al. 2003; Bekki & Chiba 2004), which suggests that the adopted assumption is quite reasonable.

We perform purely dissipationless simulations on galaxy-scale halo formation via hierarchical merging of subhalos with field stars and GCs. In these dissipationless simulations, we first identify possible formation sites of field stars and GCs in low-mass halos at high z and then follow their evolution during hierarchical merging of the halos till $z = 0$. The final structural and kinematical properties of the stellar halo and GCS in the simulated LMC are thus determined by the details of merging histories of subhalos with field stars and GCs. We consider that as long as the formation sites of field stars and GCs in low-mass halos are properly modeled, the present dissipationless models allow us to derive physical properties of the stellar halo and the GCS in the LMC in a reasonable way. The present simulations are different from our previous chemodynamical ones (Bekki & Chiba 2000; 2001) which investigated both dynamical and chemical evolution of forming galaxies in order to reproduce structures, kinematics, and chemical properties *for the Galactic field stars* in a self-consistent manner. We consider that it is currently difficult and numerically costly to construct the fully self-consistent chemodynamical models in which formation sites *both for field stars and GCs* can be *directly* derived for gaseous regions of low-mass halos. Accordingly, the present study is the first step for better modeling star and GC formation in the LMC. Fully self-consistent chemodynamical simulations with reasonable and realistic models for star and GC formation from GMCs will be done in our future works.

2.2 Identification of field star and GC particles in hierarchical galaxy formation

We simulate the formation of galaxy-scale halos in a Λ CDM Universe with $\Omega = 0.3$, $\Lambda = 0.7$, $H_0 = 70 \text{ km s}^{-1} \text{ Mpc}^{-1}$, and $\sigma_8 = 0.9$, and thereby investigate merging/accretion histories of subhalos that can contain low mass dwarfs. The way to set up initial conditions for the numerical simulations is essentially the same as that adopted by Katz & Gunn (1991) and Steinmetz & Müller (1995). We consider an isolated homogeneous, rigidly rotating sphere, on which small-scale fluctuations according to a CDM power spectrum are superimposed. The initial total mass (M_t), radius, initial overdensity (δ_i), and spin parameter (λ) are set to be free parameters.

Although we investigate variously different models with $6 \times 10^9 M_\odot \leq M_t \leq 6.0 \times 10^{11} M_\odot$, $\lambda = 0.08, 0.12$, and 0.16 , and $\delta_i = 0.19$ and 0.39 , we mainly show the results of the “LMC” models with $M_t = 6.0 \times 10^{10} M_\odot$ and $\lambda = 0.08$. The choice of $\lambda = 0.08$ are demonstrated to be quite reasonable for late-type disk galaxies in previous CDM simulations (e.g., Katz & Gunn 1991; Steinmetz & Müller 1995; Bekki & Chiba 2000, 2001), and accordingly we consider that models with $\lambda = 0.08$ are also reasonable for the present simulations for less luminous disk systems like the LMC. $\delta_i = 0.39$ is chosen such that the final central velocity dispersions of “stellar” components are similar to the observed ones.

The low-mass ($M_t = 6 \times 10^9 M_\odot$) models show stellar

halos with velocity dispersions being significantly lower than the observed one. The high-mass ($M_t = 6 \times 10^{11} M_\odot$) models are investigated in order that we can compare the results of the LMC model with those of “the Galaxy” one and thereby discuss the differences in dynamical properties between the LMC’s GCS and the Galactic GCS. These results will be discussed in a wider context of stellar halo and GCS formation in galaxies with different Hubble types (Bekki & Chiba 2007, in preparation). The details of parameter values in the simulations including those related to simulation methods (e.g., softening lengths) are described later.

We start the collisionless simulation at $z_{\text{start}} (=30)$ and follow it till $z_{\text{end}} (=1)$ to identify virialized subhalos with the densities larger than $170\rho_c(z)$, where $\rho_c(z)$ is the critical density of the universe, at a redshift z . This $170\rho_c(z)$ corresponds to the mean mass density of a collapsed and thus gravitationally bound object at z (e.g., Padmanabhan 1993). The minimum number of particles within a virialized subhalo (N_{min}) is set to be 32 corresponding to the mass resolution of $3.8 \times 10^6 M_\odot$ for the LMC models. This number of 32 is chosen so that we can find a virialized object at a given z in a robust manner. The mass resolution of $1.2 \times 10^5 M_\odot$ is chosen such that the masses of GC particles in the simulations can be consistent with the observed typical GC mass ($\sim 10^5 M_\odot$) in the Galaxy.

For each individual virialized subhalo with the virialized redshift of z_{vir} , we estimate a radius (r_b) within which 20 % of the total mass is included, and then the particles within r_b are labeled as “baryonic” particles. This procedure for defining baryonic particles is based on the assumption that energy dissipation via radiative cooling allows baryon to fall into the deepest potential well of dark-matter halos. Such baryonic particles in a subhalo will be regarded as candidate “stellar” particles to form stellar halos and GCSs in the later dynamical stage, if the subhalo is later destroyed and baryonic particles initially within the subhalo is dispersed into the galactic halo region. Thus, the present dissipationless models track the formation of stellar halos and GCSs via hierarchical merging of subhalos, although the models are not adequate to the study of star formation histories in subhalos (as was done in our previous studies, e.g., Bekki & Chiba 2001).

Stellar particles within r_b in a subhalo are divided into field star (“FS”) particles and “GC” ones accordingly to their locations with respect to the center of the subhalo. The stellar particle in the very center of a subhalo is identified as GC particle whereas stellar particles other than the GC particle within r_b are identified as FS ones. The initial distributions of FS particles are thus more diffuse than those of the GC particles in virialized subhalos. Massive, compact star clusters like GCs are suggested to be formed in extraordinary high-pressure regions, such as the centers of low-mass galaxies (e.g., Elmegreen 2004). Unbound or weakly bound star clusters, which can evolve into field stars after their disintegration, can be formed in outer regions of galaxies where gas density and pressure are low (e.g., Elmegreen 2004). We thus consider that the adopted model for the distributions of the two old stellar components is reasonable. The differences in initial positions with respect to the centers of subhalos between FS and GC particles can cause differences in the final distribution with respect to a galaxy-scale halo formed from the subhalos between these particles.

In the present model, each subhalo is assumed to have only one GC particle that is located in the center of the halo. One of the main reasons for this is that GCs in the present simulations are considered to be formed in nuclear regions of low-mass halos (i.e., GCs are initially either nuclear star clusters or stellar galactic nuclei): this assumption is similar to the scenario proposed by Zinnecker et al. (1988). Furthermore, our analytical arguments suggest that low-mass dark halos with the masses of $2 \times 10^8 M_\odot$, the luminous masses being 10% of the halos, and specific frequencies of GCs being 5 can have one GC. Given that the halos identified as being virialized before reionization at each time step in the simulations mostly have masses less than $2 \times 10^8 M_\odot$, the above assumption of one GC in a halo can be reasonable.

If the initial number of GC particles in each halo is increased, the initial difference in spatial distributions between halo and GC particles becomes less remarkable in the halo: the final differences in structural and kinematical properties between the stellar halo and the GCS in the LMC therefore becomes less remarkable. Thus the adopted models with each subhalo having only one nuclear GC particle is regarded as those showing maximum possible differences in final dynamical properties between the stellar halo and the GCS in the present LMC model.

2.3 Truncation of GC formation

Previous theoretical studies have demonstrated that ultraviolet background radiation in a reionized universe can significantly reduce the total amount of cold HI and molecular gas that are observed to be indispensable for galactic active star formation (e.g., Susa & Umemura 2004). In order to investigate this suppression effects of star and GC formation on the final structural and kinematics properties of the simulated stellar halos and GCSs, we adopt the following idealized assumption: *If a subhalo is virialized after the completion of the reionization (z_{reion}), star and GC formation is totally suppressed in such a subhalo.* Then, hypothetical baryonic/stellar particles in the subhalos with $z_{\text{vir}} < z_{\text{reion}}$ will *not* be identified as FS or GC particles in the later stage, but those in the subhalos with $z_{\text{vir}} \geq z_{\text{reion}}$ will be regarded as progenitors of visible stellar halos.

Recent WMAP (*Wilkinson Microwave Anisotropy Probe*) observations have shown that plausible z_{reion} ranges from 11 to 30 (Spergel et al. 2003; Kogut et al. 2003) whereas quasar absorption line studies give the lower limit of 6.4 for z_{reion} (Fan et al. 2003). Guided by these observations, we investigate the models with $z_{\text{reion}} = 0$ (no reionization), 6, 10, 15, and 20. The adopted picture of single epoch of reionization might well be somewhat oversimplified and less realistic, however, this idealized model can help us to elucidate some essential ingredients of the reionization effects on stellar halo and GC formation. For convenience, the epoch of the truncation of GC formation by reionization is denoted as z_{trun} in the following.

We show the results of the models with $z_{\text{trun}} = 10$ and 15, firstly because these models explain structural properties of the Galactic stellar halo and GCS (Bekki 2005; Bekki & Chiba 2005) and secondly because models with higher z_{trun} can also better explain the observed properties of GCSs in early-type galaxies (Bekki et al. 2007). Furthermore, the adopted higher z_{trun} are roughly consistent with the latest

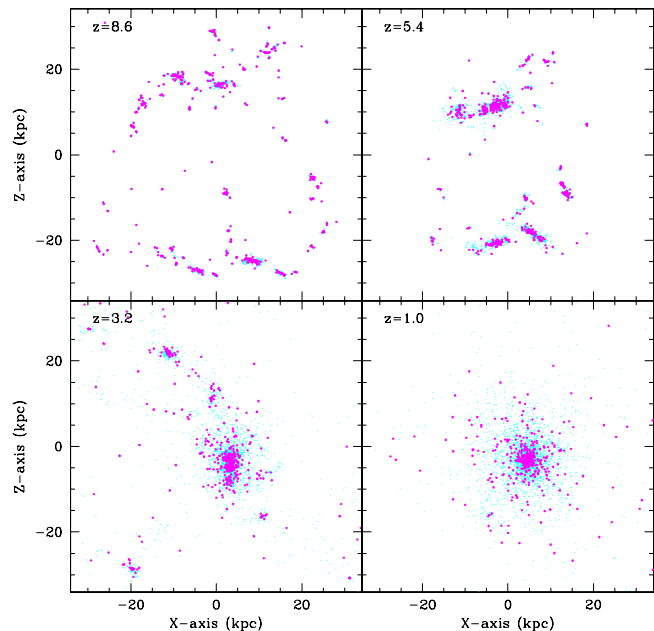


Figure 1. Time evolution of spatial distributions of “FS” (field star) particles (cyan) and “GC” (globular cluster) ones (magenta) projected onto the x - z plane in the standard LMC model. For clarity, GC particles are plotted by bigger dots. The redshift (z) is given in the upper left corner for each panel.

observation by WMAP suggesting that the epoch of reionization is $z = 10.9^{+2.7}_{-2.3}$ (Page et al. 2006). The models with $z_{\text{trun}} < 10$ are found to yield too many GCs (> 1000) in the present models so that they can not be consistent with the observed number of old GCs (13) in the LMC. Therefore, we mainly discuss the results of the models with $z_{\text{trun}} = 15$ in the present study.

It should be stressed here that without truncations of GC formation after reionization, the present models produce too many GCs owing to a large number of low-mass halos virialized after reionization so that they can not be consistent with observations. This however does not necessarily mean that the truncation of GC formation by reionization is a crucial in better understanding the origin of the LMC’s GCS: later, selective dynamical destruction of low-density GCs originating from low-density halos virialized *after reionization* might well dramatically reduce the overproduced GCs in a model with no truncation of GC formation by reionization so that the simulated GC number can be consistent with the observed one even in such a model. Such later destruction of GCs is not modeled at all in the present study.

2.4 Main points of analysis

We investigate final structural and kinematical properties of stellar halos and GCs at $z = 1$ in models with different model parameters. We note that later accretion of satellites at $z < 1.5$ is minor in the final structures of the simulated halos at $z = 0$, so the calculation is ended at $z_{\text{end}} = 1$ to obtain the dynamically relaxed halo structures. We first show the “standard” LMC model with $M_t = 6.0 \times 10^{10} M_\odot$,

$\delta_i = 0.39$, $\lambda = 0.08$, and $z_{\text{trun}} = 15$ then discuss parameter dependences of the results.

We adopt the initial LMC mass significantly larger than that of $2 \times 10^{10} M_\odot$ used in the latest simulations for the orbital evolution of *the present* LMC interacting with the SMC (e.g., Yoshizawa & Noguchi 2003). The reason for this is that numerical simulations demonstrated that the mass of the LMC can become significantly smaller than its initial mass owing to stripping of dark matter halo and stars by the Galactic tidal field (Bekki & Chiba 2005): We need to adopt the LMC’s mass significantly larger than the present LMC mass. The standard model shows that (1) the final mass within 7.5 kpc is about $2 \times 10^{10} M_\odot$ and (2) the central velocity dispersion of the stellar halo is $50 - 60 \text{ km s}^{-1}$ depending on projections. Models with smaller initial masses ($\sim 10^{10} M_\odot$) shows that final velocity dispersions of stellar halos are significantly smaller than the observed one.

Although the derived kinematics in the standard model is roughly consistent with observations (e.g., Minniti et al. 2003), we investigate the following three models for comparison: The “low density” model with $\delta_i = 0.19$, the “high threshold” one with $N_{\text{min}} = 1000$, and the “low- z truncation” one with $z_{\text{trun}} = 10$. The velocity dispersion of the stellar halo in the low density model ($30 - 40 \text{ km s}^{-1}$) is significantly smaller than the observed one, because the final single halo has a lower mean density and thus have a smaller mass at $z = 1$ within 20 kpc that is more reasonable for the tidal radius in the more massive LMC at $z = 1$ than the present tidal radius of 15 kpc (van der Marel et al. 2002). Only subhalos with masses larger than $10^8 M_\odot$ at the epochs of virialization can have FSS and GCs in the high threshold model.

By assuming that the projected radial density profiles of GCSs (Σ_{GC}) are described as the power-law form;

$$\Sigma_{\text{GC}} \propto R^\alpha, \quad (1)$$

we derive the power-law slope (α) for each GCS. The derived power-law slopes can be compared with those of stellar halos with $\Sigma_{\text{FS}} \propto R^\alpha$ so that we can discuss the differences in structural properties of these two old stellar components. The maximum velocities (V_m) and the central velocity dispersion (σ_0) in the radial dependences of rotational velocities (V_{rot}) and velocity dispersions (σ) are derived to discuss kinematics of the two components. For convenience, V_m/σ_0 is simply referred to as V/σ throughout this paper.

We adopt the slit size of 5 kpc (corresponding to the effective radius of the simulated GCS) so that we can estimate the radial profiles of V_{rot} and σ with reasonably small error bars. Errors in V_{rot} (σ) are assumed to be equal to $V_{\text{rot}}/\sqrt{2(N-1)}$ ($\sigma/\sqrt{2(N-1)}$), where N is the total number of particles for a given radial bin. Errors in V/σ are estimated from the total number of particles at the radii where V_{rot} becomes maximum.

The total number of GCs are $70 - 450$ (at $z = 1$) in the models with $z_{\text{trun}} = 15$ and thus much larger than the observed number (13) of old GCs in the present LMC. McLaughlin (1999) showed that total number of initial GCs in a galaxy can decrease by a factor of 25 within the Hubble time owing to GC destruction by the combination effect of galactic tidal fields and internal GC evolution (e.g., mass loss from massive and evolved stars). Therefore, it is reasonable to say that only several percent of the simulated GCs

can survive to be observed as halo GCs in the LMC. We thus consider that the above range of GC number can be reasonable to be compared with observations.

Table 1 summarizes the parameter values: Model name (column 1), M_t (2), λ (4), δ_i (3), N_{min} (5), z_{trun} (6), $(\frac{V}{\sigma})_{\text{FS}}$ (7), and $(\frac{V}{\sigma})_{\text{GC}}$ (8). Here $(\frac{V}{\sigma})_{\text{FS}}$ ($(\frac{V}{\sigma})_{\text{GC}}$) is the mean V/σ for the three projections (x - y , x - z , and y - z) for the stellar halo (GCS). Our previous simulations of disk galaxy formation shows that the final spin vectors of the simulated disks are similar to the initial spin vectors of dark matter halos (Bekki & Chiba 2001). We thus consider that the x - z plane of the simulated LMC corresponds to the disk plane of the LMC in order to discuss the observed kinematics of the stellar halo and the GCS.

All the calculations have been carried out on the GRAPE board (Sugimoto et al. 1990). Total number of particles used in our simulations is 508686 and the gravitational softening length is 0.18 kpc for the LMC models. The adopted softening length is roughly similar to the initial mean separation of the particles in a simulation. We used the COSMICS (Cosmological Initial Conditions and Microwave Anisotropy Codes), which is a package of fortran programs for generating Gaussian random initial conditions for nonlinear structure formation simulations (Bertschinger 1995).

The present study does not intend to investigate destruction of GCs and the resultant formation of field stars in the LMC’s halo. The halo field stars originating from low-mass GCs and initially unbound or weakly bound star clusters (SCs) may well have structural and kinematical properties similar to those of the GCS in the LMC, if the probability of GCs (and SCs) being destroyed by the combination effects of the LMC’s tidal field and internal GC evolution does not depend on orbits of GCs with respect to the LMC’s center. As described later, the simulated halo and GCS in the LMC have similar dynamical properties. Thus, field halo formation via GC destruction would not change the main results of the present models.

As described later, the present models do not reproduce self-consistently the observed kinematics of halo field stars and GCs in the LMC. This is in a striking contrast with previous simulations (e.g., Santos 2003; Bekki 2005) in which physical properties of the Galactic GCS can be well reproduced if truncation of GC formation by reionization is properly modeled. This is partly because the previous simulations only tried to explain the Galactic GCS, where remarkable kinematical differences in halo field stars and GCs are not observed (i.e., they did not discuss stellar halos and GCSs in less luminous galaxies like the LMC).

3 RESULTS

3.1 The standard model

Figure 1 shows the time evolution of spatial distributions of FSS and GCs from $z = 30$ to $z = 1$ that are formed within subhalos virialized before $z = z_{\text{trun}}$ ($=15$). 434 small subhalos are virialized before $z = z_{\text{trun}}$ and have masses less than $3.0 \times 10^7 M_\odot$ at the virialization and grow via hierarchical merging with other subhalos with and without FSS and GCs ($z = 8.6$). These smaller subhalos with FSS and GCs

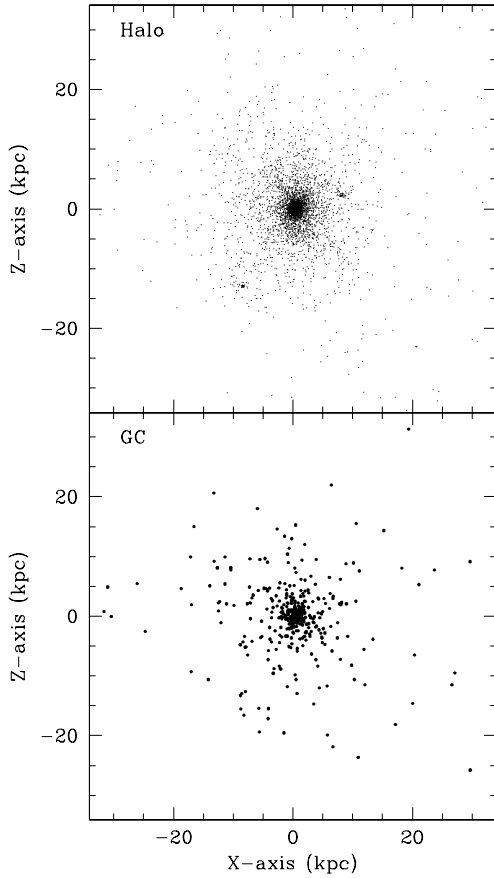


Figure 2. The final distributions of FS particles (upper) and GC ones (lower) projected onto the x - z plane in the standard model at $z = 1$. FS and GC particles form the stellar halo and the GCS, respectively, in the present study. The GCS appears to be slightly flattened in comparison with the stellar halo owing to the smaller number of GC particles with $|z| > 20$ kpc. The overall distributions are however quite similar with each other in this model.

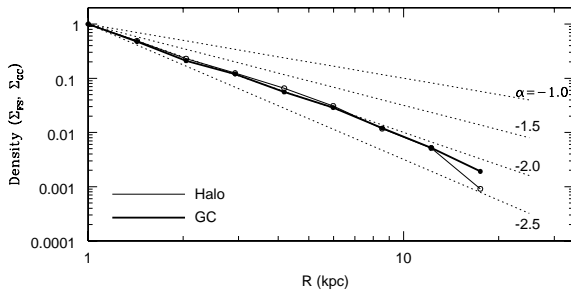


Figure 3. The final projected radial profiles of FS (thin solid) and GC (thick solid) particles in the standard model. For comparison, the profiles normalized to their central values are shown. Both profiles can be well described as power-law ones with the slopes $\alpha \sim -2.0$ for $R < 10$ kpc.

merge with one another to form bigger subhalos ($z = 5.4$), and finally these bigger halos also merge with one another ($z = 3.2$) to form a single halo till $z = 1$. FSs and GCs are tidally stripped from the subhalos during this hierarchical merging and consequently dispersed into the halo region to form a stellar halo and a GCS.

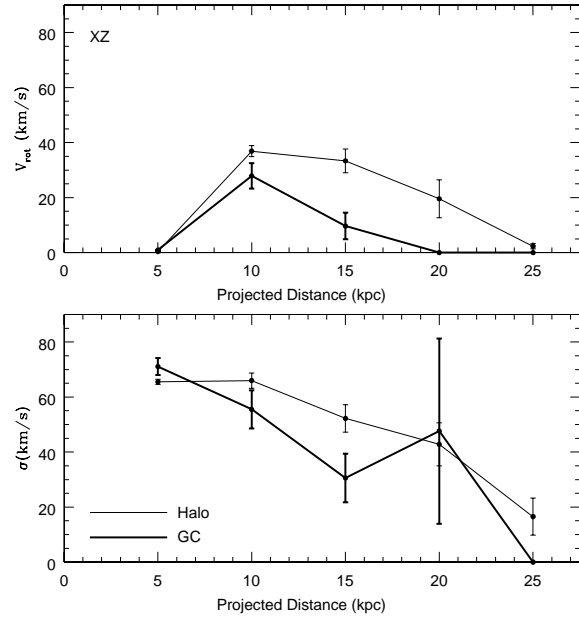


Figure 4. Radial dependences of rotational velocities V_{rot} (upper) and velocity dispersions σ (lower) for the stellar halo (thin solid) and the GCS (thick solid) projected onto the x - z plane in the standard model with the slit size of 5 kpc for the estimation of V_{rot} and σ in each bin. The projected distance here means the distance along the x -axis in the simulation (See Figure 2). The results are shown for $0 \text{ kpc} \leq x \leq 25 \text{ kpc}$ in the V_{rot} profile and for all selected particles with $|x| \leq 25 \text{ kpc}$ in the σ one. $V_{\text{rot}} = 0$ are plotted with no error bars for bins with no GC particles (e.g., at $x \approx 25 \text{ kpc}$). Although the error bars are not small, it is clear that both the stellar halo and the GCS show little rotation.

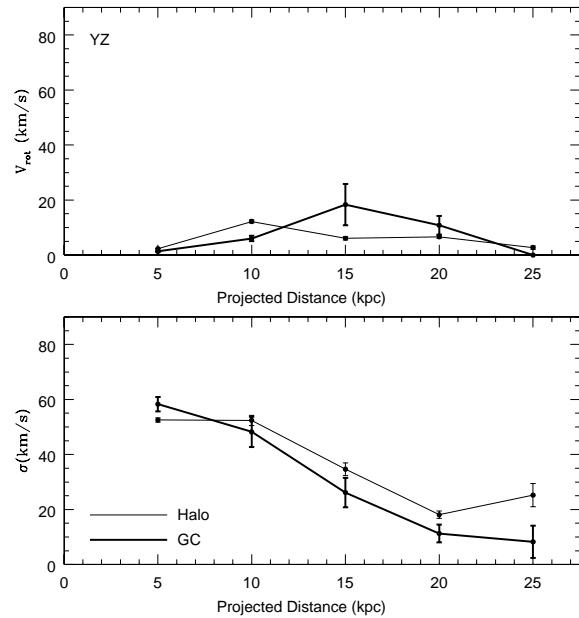


Figure 5. The same as Figure 4 but for the halo and the GCS projected onto the y - z plane in the standard model.

Figure 2 shows that both the stellar halo (composed of FSs) and the GCS (GCs) have similar spherical distributions in the x - z projection, though the GCSs has a smaller number of GCs with $|z| > 20$ kpc. There are no significant differences in distributions projected onto the x - y , x - z , and y - z planes between the two components: both components show flattened distributions in the three projections with the major axes aligned with each other. These similarities means that the internal structures between the two components are almost identical. The half-number radius is 5.0 kpc for the stellar halo and 5.3 kpc for the GCS, which suggests that there are no significant differences in dynamical properties between these two components.

Figure 3 shows that both the stellar halo and the GCS have radial density profiles that can be approximated by the power-law ones with the slopes of $\alpha \sim -2$ at least for $R < 20$ kpc. The apparent lack of flattening in the profile of the stellar halo in the inner part of the simulated LMC ($R < 2$ kpc) is inconsistent with the best-fit exponential profile by Alves (2004), which shows flattening (or “core”) of the profile for $R < 1$ degree from the LMC’s center. Although this inconsistency between the simulated and the observed halos of the LMC has some profound physical meanings about the formation processes of the stellar halo (Bekki & Chiba 2007, in preparation), we intend to discuss this not in this paper but in our future papers.

Figures 4 and 5 show that there are no remarkable differences in the radial dependences of rotational velocities (V_{rot}) and velocity dispersions (σ) between the stellar halo and the GCS. Both components show overall small V_{rot} ($< 40 \text{ km s}^{-1}$), radially decreasing σ profiles, and small V/σ (< 0.6). The estimated V/σ in the x - y , x - z , and y - z projections are 0.25 ± 0.18 , 0.57 ± 0.13 , and 0.21 ± 0.01 , respectively, for the stellar halo, and 0.47 ± 0.33 , 0.60 ± 0.10 , and 0.31 ± 0.13 , respectively, for the GCS. The derived small V/σ clearly indicates that both components are dynamically supported by velocity dispersion rather than by global rotation. The results shown in Figures 3, 4, and 5 thus show that there are no significant differences in dynamical properties between the two components, though they originate from different parts of subhalos virialized before $z = z_{\text{trun}}$.

The GCS is formed from subhalos with different masses and epochs of virialization so that the spatial distributions of GCs originating from different subhalos are different with one another. For example, GCs from subhalos with masses more than $10^7 M_{\odot}$ at their virialization epochs have a half-number radius of 3.5 kpc and thus a more compact spatial distribution in comparison with the GCS composed of all GCs. Such a more compact distribution can be seen in the stellar halo composed only of FSs originating from more massive subhalos. These results imply that stellar components formed in more massive subhalos at high z are more likely to be the inner parts of galaxies at $z = 0$.

3.2 Parameter dependences

The dependences of structural and kinematical properties of stellar halos and GCSs on model parameters are summarized as follows.

(i) low-density model: Figure 6 shows that the final projected distributions of the stellar halo and the GCS in the low-density LMC model with $\delta_0 = 0.19$ appears to be flat-

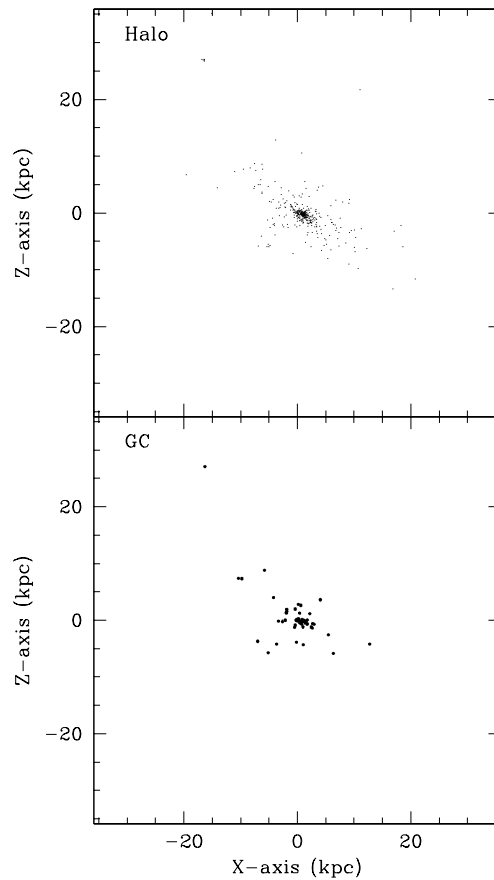


Figure 6. The same as Figure 2 but for the low-density LMC model. Note that both the stellar halo and the GCS appear to be flattened.

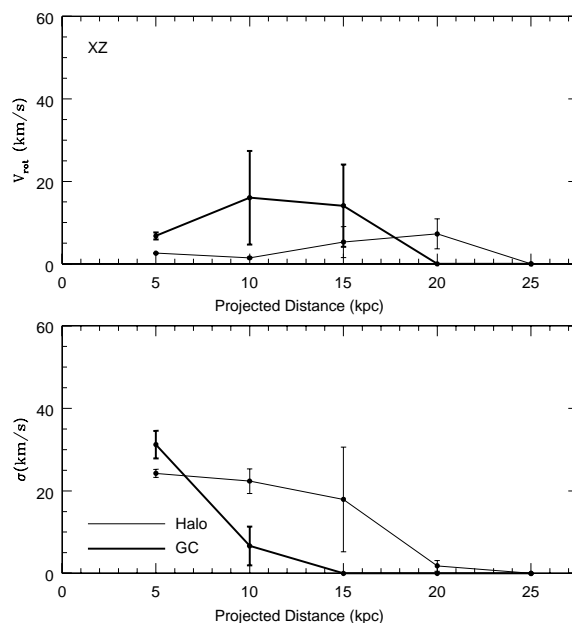


Figure 7. The same as Figure 4 but for the low-density LMC model. $V_{\text{rot}} = 0$ ($\sigma = 0$) are plotted with no error bars for bins with no GC (or halo) particles (e.g., $x \approx 20$ kpc and $x \approx 25$ kpc in the V_{rot} profile of GCs).

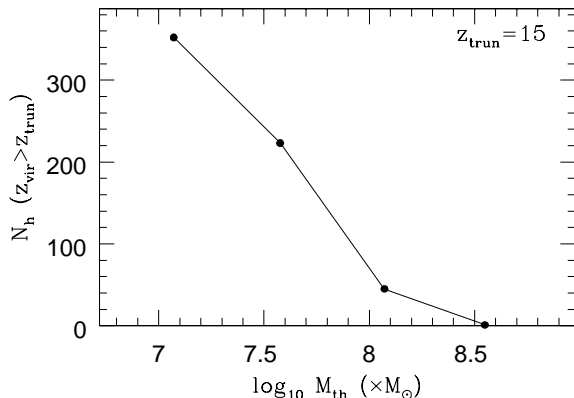


Figure 8. The dependence of the total number of subhalos (N_h) with GCs, $z_{\text{vir}} > z_{\text{trun}}$, and $M_h > M_{\text{th}}$ in the standard model with different M_{th} for $z_{\text{trun}} = 15$. M_h is the mass of a halo when the halo is identified as a “virialized system” in the simulation. Note that N_h is very small for $M_{\text{th}} > 3 \times 10^8 M_{\odot}$.

tened in comparison with the standard model. We confirm that this flattening can be seen in the three projections (i.e., x - y , x - z , and y - z) and thus suggest that the derived flattening is due to the lower initial density of the LMC in this model. The power-law slope α in the projected density distribution is -2.5 both for the stellar halo and for the GCS, which means that the radial density profiles are slightly steeper in this model than in the standard one.

(ii) low-density model: Figure 7 shows that the two components in the low-density model have a small amount of rotation ($V_{\text{rot}} < 20 \text{ km s}^{-1}$), which suggests that the two components are dynamically supported by velocity dispersion. The mean V/σ is 0.60 for the stellar halo and 0.56 for the GCS, which are slightly higher than those in the standard model (See table 1). Flattened shapes and small V/σ in this model suggest that the two components have anisotropic velocity dispersions.

(iii) high N_{min} model: the high threshold model with $N_{\text{min}} = 1000$ has more compact distributions of the stellar halo and the GCS with the half-number radii of the two equal to 4.5 kpc and 3.4 kpc, respectively. This is due to the fact that more massive subhalos virialized before z_{trun} can finally settle in the inner region of the LMC in this model. The GCS appears to be more flattened than the stellar halo, though V/σ is not different between the two components.

(iv) low- z truncation model: both the stellar halo and the GCS have less compact spatial distributions and shallower radial density profiles with $\alpha \sim -1.5$ for the central 10 kpc in the low- z truncation model. Both the stellar halo and the GCS have small V/σ (0.19 and 0.21, respectively), which means that the two components are supported by velocity dispersion more strongly. A large number of GCs (~ 5000) is totally inconsistent with observations, even if later GC destruction by galactic tidal fields are considered.

(v) Thus the present models all show very small V/σ (0.2 – 0.6) of GCSs, which is much smaller than the observed value of ~ 2 . Small V/σ can be seen in models with high spin parameters (e.g., $\lambda = 0.12$) and low initial masses ($M_t = 2.0 \times 10^{10} M_{\odot}$) and thus suggests that the present *dissipationless* models can not reproduce well the observed rotational kinematics of the LMC’s GCS. The inner flat-

tened halo derived only in the low-density model can be consistent with the observed one by Subramaniam (2006) and thus implies that the LMC could be formed from a low-density galaxy-scale fluctuation.

4 DISCUSSIONS

We have shown that (1) there are no significant kinematical differences in the simulated stellar halos and GCSs in the LMC models and (2) V/σ of the GCSs can not be as high as observed (~ 2) in the GCS of the LMC. These failures to reproduce the observed kinematical differences between the two old stellar components (i.e., stellar halo and GCS) in the LMC imply that the adopted models for the formation of the two components at high redshifts can lack some important ingredients of GC formation. These failures can be due to the adopted assumptions that (i) all subhalos with different masses and different redshifts of virialization can have *both field stars and GCs* and (ii) the GCS was formed from *dissipationless merging* of subhalos that had been virialized before reionization (i.e., $z_{\text{vir}} > z_{\text{trun}}$) and thus had GCs (before their merging leading to the formation of the LMC at later redshifts).

Observational studies of GCs for galaxies in the Local Group of galaxies showed that dwarf galaxies fainter than $M_V = -13$ mag appear to have no GCs (van den Bergh 2000). This result means that (i) there could be a possible threshold galaxy mass ($10^8 - 10^9 M_{\odot}$) above which GC formation is possible and (ii) the present dissipationless models discussed so far did not consider this possible threshold mass (M_{th}). We accordingly investigate how the total number of subhalos that can be virialized before z_{trun} and thus have GCs (N_h) depend on M_{th} for the standard model with $z_{\text{trun}} = 15$. Figure 8 shows that (i) N_h is smaller for the models with larger M_{th} and (ii) if $M_{\text{th}} > 3 \times 10^8 M_{\odot}$, almost no subhalos virialized before $z_{\text{trun}} = 15$ can have GCs. The required M_{th} for no halo formation with GCs before reionization is higher for lower z_{trun} .

These results in Figure 8 therefore imply that if there is a threshold halo mass (M_{th}) for GC formation and if $M_{\text{th}} > 3 \times 10^8 M_{\odot}$, the LMC’s GCS can not be formed from hierarchical merging of subhalos with $z_{\text{vir}} > z_{\text{trun}}$ and with GCs. As shown in the present studies, dissipationless merging of subhalos is responsible for the larger velocity dispersion of old stellar components. These results in Figure 8 accordingly imply that the observed small velocity dispersion of the LMC’s GCS is due to the fact that the LMC’s GCS was not formed from dissipationless merging of low-mass subhalos with $z_{\text{vir}} > z_{\text{trun}}$. Figure 8 thus implies that old, metal-poor GCs in the LMC were not formed in low-mass subhalos that were the building blocks of the LMC, because the masses of the subhalos were systematically lower than M_{th} before reionization.

If the LMC’s old GCs do not originate from subhalos virialized at high redshifts, how were they formed? Previous numerical simulations showed that GCs can be formed during dissipative merging between the Galaxy and gas-rich dwarfs (Bekki & Chiba 2002). We accordingly consider that *dissipative merging* of gas-rich subhalos can trigger the formation of GCs at the very early epoch of the disk formation of the LMC. Formation of GCs via dissipative merg-

ing of subgalactic clumps (e.g., gas-rich dwarfs) in the very early epoch of galactic disk formation results in disky spatial distributions and rotational kinematics of GCSs (Bekki & Chiba 2002). If old, metal-poor GCs in the LMC are formed by the above dissipative processes, they should have slightly younger ages than the Galactic counterparts.

We thus suggest the following possible scenario for the origin of the observed kinematical difference in the stellar halo and the GCS of the LMC: (1) the stellar halo was formed from merging of low-mass subhalos with field stars and with no/few GCs (i.e., GC-less galaxy building blocks) and thus shows a large velocity dispersion and a low V/σ and (2) the GCS was formed through dissipative merging of gas-rich subhalos and gas infall at the very early epoch of the disk formation and thus shows rotational kinematics. In the first part (1) of this scenario, the masses of subhalos virialized before reionization were well below the threshold mass (M_{th}) for GC formation so that the halos could not form GCs. We thus suggest that M_{th} can cause differences in structural and kinematical properties between stellar halos and old GCs in less luminous galaxies like the LMC.

Olsen et al. (2004) found that the kinematics of GCSs in late-type galaxies in the Sculptor group are consistent with rotational kinematics seen in HI components of these galaxies and suggested that the GCSs were formed in disks rather than in halos. Beasley et al. (2006) also found a large $V/\sigma \sim 3$ of the GCS in the low-mass dwarf galaxy (VCC 1087) in the Virgo cluster of galaxies. These observations imply that the rotational kinematics seen in the LMC's GCS is not exceptional but can be found in GCSs of many less luminous galaxies and thus that the formation processes of GCSs in these galaxies can be discussed in terms of the proposed scenario above. We also suggest that there can be two different formation processes of old, metal-poor GCs before and after reionization: one is GC formation in high-density central regions of subhalos early virialized before reionization and the other is GC formation in the very early stage of disk formation. Future observational studies on the shapes of the stellar halos in these galaxies with GCSs having rotational kinematics will enable us to discuss the origin of the possible differences in structures and kinematics between the stellar halos and the GCSs for these galaxies in the context of the proposed scenario.

5 CONCLUSIONS

We numerically investigated structural and kinematical properties of the stellar halo and the GCS in the LMC by assuming that the two old components can be formed from dissipationless merging of subhalos that were virialized before reionization and contained both field stars and GCs. We particularly discussed whether or not the observed GCS's rotational kinematics ($V/\sigma \sim 2$) can be reproduced by the present models. Our simulations with different model parameters showed that the GCS composed of metal-poor GCs formed high redshifts ($z > 6$) before reionization has little rotation ($V/\sigma \sim 0.4$) and structures and kinematics similar to those of the stellar halo. This inconsistency therefore implies that if old, metal-poor GCs in the LMC have rotational kinematics, they are highly unlikely to originate from the low-mass subhalos that formed the stellar halo:

the adopted assumption that both the field stars and the GCs in the LMC were formed within *all low-mass subhalos* virialized before reionization is highly likely to be wrong.

We accordingly considered that there could be a threshold halo mass (M_{th}) above which GCs can be formed (i.e., below which only field stars can be formed) and investigated how the number of subhalos (N_{h}) that can be virialized before z_{run} and have GCs depends on M_{th} for $z_{\text{run}} = 15$. We found that if $3 \times 10^8 M_{\odot} \leq M_{\text{th}}$, the present LMC can not contain GCs formed within subhalos with the redshifts of their virialization (z_{vir}) larger than that of reionization (z_{run}). We also suggested that if z_{run} is lower, the required M_{th} (for no GC formation) needs to be higher. We therefore concluded that if old, metal-poor GCs in the LMC have rotational kinematics, they were not formed in subhalos virialized before reionization.

We suggested a possible scenario in which the stellar halo was formed from low-mass subhalos virialized before reionization and having no/few GCs whereas the GCS was formed at the very early epoch of the disk formation via dissipative merging of gas-rich subhalos and gas infall well after reionization. In this scenario, the origin of the observed possible rotational kinematics of the LMC's GCS is closely associated with dissipative gas dynamics in the disk formation of the LMC. The LMC's GCs are thus suggested to be slightly younger than the Galactic counterparts. It is however unclear how old GCs can be formed during dissipative formation of the main body of the LMC. We thus plan to investigate whether the observed possible global rotation of the GCS in the LMC can be reproduced by our more sophisticated numerical models with gas dynamics and GC formation.

We also suggested that the threshold halo mass (M_{th}) for GC formation can cause significant differences in structural, kinematical, and chemical properties between stellar halos and GCSs in less-luminous galaxies like the LMC. Future observations will extensively investigate structural and kinematical differences in stellar halos and GCs for galaxies beyond the Local Group and thus confirm the presence or the absence of the differences. We plan to investigate dependences of physical properties of stellar halos and GCSs on physical conditions of their host galaxies at their formation epochs (e.g., masses and spin parameters) based on fully self-consistent chemodynamical simulations.

ACKNOWLEDGMENTS

We are grateful to the referee for valuable comments, which contribute to improve the present paper. KB acknowledges Masashi Chiba for his useful discussions on the origin of stellar halos in galaxies. KB acknowledges the financial support of the Australian Research Council throughout the course of this work. The numerical simulations reported here were carried out on GRAPE systems kindly made available by the Astronomical Data Analysis Center (ADAC) at National Astronomical Observatory of Japan (NAOJ).

REFERENCES

Alves, D. R., 2004, ApJ, 601, L151

- Beasley, M. A., Strader, J., Brodie, J. P., Cenarro, A. J., Geha, M., 2006, *AJ*, 131, 814
- Bekki K., 2005, *ApJ*, 626, L93
- Bekki, K., Chiba, M., 2000, *ApJ*, 534, L89
- Bekki, K., Chiba, M., 2001, *ApJ*, 558, 666
- Bekki, K., Chiba, M., 2002, *ApJ*, 566, 245
- Bekki, K., Chiba, M., 2004, *A&A*, 417, 437
- Bekki, K., Chiba, M., 2005, *MNRAS*, 356, 680
- Bekki, K., Couch, W. J., Beasley, M. A., Forbes, D. A., Chiba, M., Da Costa, G., 2004, 610, L93
- Bekki, K.; Freeman, K. C., 2003, *MNRAS*, 346L, 11
- Bekki, K., Yahagi, H., Forbes, D. A., 2007, *MNRAS*, 377, 215
- Bertschinger, E., 1995, *astro-ph/9506070*
- Borissova, J., Minniti, D., Rejkuba, M., Alves, D., 2006, *A&A*, 460, 459
- Brodie, J. P., Strader, J., 2006, *ARA&A* in press (*astro-ph/0602601*)
- Chiba, M., Beers, T. C., 2001, *ApJ*, 549, 325
- Cioni, M.-R. L., Habing, H. J. 2003, *A&A*, 402, 133
- Cole, A. A., Smecker-Hane, T. A., Gallagher, J. S., III., 2000, *AJ*, 120, 1808
- Elmegreen, B. G., 2004, in *The Formation and Evolution of Massive Young Star Clusters*, eds. H.J.G.L.M. Lamers, L.J. Smith, and A. Nota. i(San Francisco: ASP), ASP Conf. Ser. 322, p.277
- Elmegreen, B. G. Efremov, Y. N., 1997, *ApJ*, 480, 235
- Fan, X. et al., 2003, *AJ*, 125, 1649
- Freeman, K. C., Illingworth, G., Oemler, A., Jr., 1983, *ApJ*, 272, 488
- Graff, D. S., Gould, A. P., Suntzeff, Nicholas B., Schommer, R. A., Hardy, E., 2000, *ApJ*, 540, 211
- Gratton, R. G., Bragaglia, A., Clementini, G., Carretta, E., Di Fabrizio, L., Maio, M., Taribello, E., 2004, *A&A*, 421, 937
- Grocholski, A. J., Cole, A. A., Sarajedini, A., Geisler, D., Smith, V. V., 2006, *AJ*, 132, 1630
- Hartwick, F. D. A., Cowley, A. P., 1988, *ApJ*, 334, 135
- Irwin, M. J., 1991, in *The Magellanic Clouds*, IAU148, ed. Raymond Haynes and Douglas Milne, Kluwer Academic Publishers, Dordrecht, p.453
- Katz, N., Gunn, J. E., 1991, *ApJ*, 377, 365
- Kennicutt, Robert C., Jr., 1998, *ARA&A*, 36, 189
- Kinman, T. D., Stryker, L. L., Hesser, J. E., Graham, J. A., Walker, A. R., Hazen, M. L., Nemec, J. M., 1991, *PASP*, 103, 1279
- Kunkel, W. E., Demers, S., Irwin, M. J., Albert, L., 1997, *ApJ*, 488, L129
- McLaughlin, D. E., 1999, *AJ*, 117, 2398
- Meatheringham, S. J., Dopita, M. A., Ford, H. C., Webster, B. L., 1988, *ApJ*, 327, 651
- Minniti, D., Borissova, J., Rejkuba, M., Alves, D. R., Cook, K. H., Freeman, K. C., 2003, *Science*, 301, 1508
- Mizutani, A., Chiba, M., Sakamoto, T., 2003, *ApJ*, 589, L89
- Olsen, K. A. G., 1999, *AJ*, 117, 2244
- Olsen, K. A. G., Salyk, C., 2002, *AJ*, 124, 2045
- Olsen, K. A. G., Miller, B. W., Suntzeff, N. B., Schommer, R. A., Bright, J., 2004, *AJ*, 127, 2674
- Padmanabhan T., 1993, *Structure Formation in the Universe*. Cambridge Univ. Press
- Page, L. et al., 2006, submitted to *ApJ* (*astro-ph/0603450*)
- Santos, M. R., 2003, in *Extragalactic Globular Cluster Systems*, Proceedings of the ESO Workshop, p. 348
- Schmidt, M., 1959, *ApJ*, 344, 685
- Schommer, R. A., Suntzeff, N. B., Olszewski, E. W., Harris, H. C., 1992, *AJ*, 103, 447
- Soszynski, I., Udalski, A., Szymanski, M., Kubiak, M., Pietrzynski, G., Wozniak, P., Zebrun, K., Szewczyk, O., Wyrzykowski, L., 2003, *AcA*, 53, 93
- Spergel, D. N. et al., 2003, *ApJS*, 148, 175
- Staveley-Smith, L., Kim, S., Calabretta, M. R., Haynes, R. F., Kesteven, M. J., 2003, *MNRAS*, 339, 87
- Steinmetz, M., & Müller, E., 1995, *MNRAS*, 276, 549
- Subramaniam, A., 2006, *A&A*, 449, 101
- Sugimoto, D., Chikada, Y., Makino, J., Ito, T., Ebisuzaki, T., Umemura, M., 1990, *Nat*, 345, 33
- Susa, H., Umemura, M., 2004, *ApJ*, 600, 1
- van den Bergh, S. 2000, *The Galaxies of the Local Group*, Cambridge: Cambridge Univ. Press.
- van den Bergh, S., 2004, *AJ*, 127, 897
- van der Marel, R. P., Cioni, M.-R. L., 2001, *AJ*, 122, 1807
- van der Marel, R. P., Alves, D. R., Hardy, E., Suntzeff, N. B., 2002, *AJ*, 124, 2639
- Yoshizawa, A., Noguchi, M., 2003, *MNRAS*, 339, 1135
- Young, L. M., Lo, K. Y., 1997, *ApJ*, 490, 710
- Zinnecker, H., Keable, C. J., Dunlop, J. S., Cannon, R. D., Griffiths, W. K., 1988, in *Grindlay, J. E., Davis Philip A. G., eds, Globular cluster systems in Galaxies*, Dordrecht, Kluwer, p603